AIP | Applied Physics Letters

Determination of electron and hole lifetimes of rutile and anatase TiO2 single crystals

Yasuhiro Yamada and Yoshihiko Kanemitsu

Citation: Appl. Phys. Lett. **101**, 133907 (2012); doi: 10.1063/1.4754831
View online: http://dx.doi.org/10.1063/1.4754831
View Table of Contents: http://apl.aip.org/resource/1/APPLAB/v101/i13
Published by the American Institute of Physics.

Determination of electron and hole lifetimes of rutile and anatase TiO_2 single crystals

Yasuhiro Yamada[1] and Yoshihiko Kanemitsu[1,2,a)]
[1]*Institute for Chemical Research, Kyoto University, Uji, Kyoto 611-0011, Japan*
[2]*JST-CREST, Sanban-cho, Chiyoda-ku, Tokyo 102-0076, Japan*

(Received 2 August 2012; accepted 12 September 2012; published online 27 September 2012)

The dynamical behavior of photoexcited states of TiO_2 governs the activities of TiO_2-based solar cells and photocatalysts. We determined the lifetimes of photoexcited electrons and holes in rutile and anatase TiO_2 single crystals by combining advantages of time-resolved photoluminescence, photoconductance, and transient absorption spectroscopy. Electrons and holes in rutile show exponential decays with the lifetime of a few tens of nanoseconds, while non-exponential decays are observed in anatase, indicating the presence of multiple carrier trapping processes. We revealed the generic features of the carrier recombination processes in rutile and anatase TiO_2. © *2012 American Institute of Physics*. [http://dx.doi.org/10.1063/1.4754831]

Titanium dioxide (TiO_2) is one of the most important oxide semiconductors in terms of energy and environmental applications, since it has been used in dye-sensitized solar cells and photocatalysts.[1,2] Much effort has recently been devoted to improving the efficiencies of solar-energy conversion and photocatalytic reactions of TiO_2-based devices through chemical substitution,[3,4] nanostructure fabrication,[5–7] surface modification,[8] and crystal structure control.[9,10] It is known that there are several stable TiO_2 polymorphs at room temperature.[11] Among them, rutile and anatase TiO_2 are the most representative ones and have been studied extensively. Although it has been discussed that anatase shows more advanced features for light–energy conversion and photocatalytic reactions than rutile,[12,13] the key factors that determine the photoactivity of TiO_2 still remain unclear.

Rutile is the most stable and dense state of the TiO_2 polymorphs. Optical absorption measurements have revealed that rutile has a direct forbidden band gap with a gap energy of 3.0 eV.[14–16] At room temperature, excitons are thermally dissociated due to the small exciton binding energy (~4 meV) and electrons (holes) behave as free carriers, while at low temperature, free exciton absorption and photoluminescence (PL) are observed.[14,15] On the other hand, anatase is metastable and has an indirect-gap structure with a 3.2 eV band-gap energy.[17–19] Both rutile and anatase are considered to have long lifetimes for electrons and holes on the basis of their band structures. The electron effective mass of anatase is smaller than that of rutile.[14,18] However, based on the analysis of optical absorption spectra and theoretical work, it has been suggested that the carriers in anatase exhibit a localizing nature due to strong electron–phonon coupling.[17,19] The similarities and differences in the optical and electronic properties of rutile and anatase have been demonstrated by many reports. However, the merits of anatase-based devices are not accounted for only by their steady-state properties, which are determined by the band structures and surface structures.

Since light–energy conversion and photocatalytic reactions are driven by photoexcited electrons and holes, it is intrinsically important to study the dynamical properties of photoexcited carriers. So far, there have been many reports on the optical responses of TiO_2, but most of them have been performed on samples in micropowder and nanoparticle forms, where the optical properties are sensitive to the fabrication method and surface treatment due to near-surface defect states. In addition, the recombination and localization processes of photogenerated electrons and holes have not been discussed well. Therefore, it is necessary to gain an understanding of the electron and hole lifetimes in the parent TiO_2 single crystals, which should lead to the development of functional and efficient TiO_2-based devices. For the study of photocarrier dynamics, the combination of different measurement techniques is necessary to determine the electron and hole lifetimes separately and check for consistency.

In this study, we investigated the photocarrier decay dynamics of rutile and anatase single crystals by combining the advantages of time-resolved PL, transient absorption (TA), and photoconductivity (PC) spectroscopy analyses to clarify the electron and hole relaxation dynamics individually and consistently. We determined the lifetimes for electrons and holes in rutile and anatase, which are essentially different from each other. In rutile, photogenerated electrons and holes show exponential decay profiles with lifetimes of 24 and 48 ns, respectively. On the contrary, in anatase, electrons and holes show nonexponential decay. In addition, the hole population decays within a few nanoseconds, while electrons persist to microseconds. Our results provide deep insights into the photoactivity of TiO_2 and offer guidelines for designing functional and efficient TiO_2-based devices.

We used commercially available rutile (Furuuchi Chemical Co. Ltd) and anatase (Crystal Base Co. Ltd.) TiO_2 single crystals. The faces of the samples, which were 0.5 mm thick, were oriented in the (100) direction. We measured the PL spectra using a monochromator and a charge-coupled-device camera. The excitation light source was an optical parametric amplifier system based on a Yb:KGW (potassium gadolinium tungstate) regenerative amplified laser with a pulse

a)Author to whom correspondence should be addressed. Electronic mail: kanemitu@scl.kyoto-u.ac.jp.

duration of 200 fs and a repetition rate of 200 kHz. Time-resolved PL measurements were performed using a streak camera and a monochromator. The time resolution of our setup was 40 ps. The PL signal was monitored at 2.8 and 2.5 eV in rutile and anatase, respectively. The laser spot size on the sample surface was measured carefully using the knife-edge method to estimate the laser excitation density. The excitation photon energy was 3.5 eV, which is well above the band-gap energies of rutile and anatase. Femtosecond TA spectroscopy was performed by a standard pump-probe technique, using a Yb:KGW-based wavelength-tunable laser system. The pump and probe energies were 3.5 and 1.2 eV, respectively. We also measured the TA decay curves in the microsecond time region using a photodiode and a digital oscilloscope. The probe light source was a continuous-wave diode laser whose photon energy was 0.9 eV, and the time resolution of this experimental setup was approximately 2 ns. For photoconductivity experiments, two Au electrodes were evaporated onto the sample surface with a separation of 150 μm, and excitation light was focused onto the gap between the electrodes. A bias voltage of 1 V was applied between the electrodes. PC dynamics were collected using a current–voltage converter and a digital oscilloscope. The TiO_2/Au interface forms the Schottky contact, whose barrier height is about 0.9 V.[20] We have confirmed that the PC dynamics is independent of the bias voltage in the range of 1–5 V, suggesting that the PC dynamics is not affected by the Schottky barrier. All the measurements were performed at room temperature.

Figure 1 shows the optical absorption, PL, and PC excitation spectra of (a) rutile and (b) anatase. PL spectra were measured under a pulse laser excitation of 250 μJ/cm^2. In rutile, strong optical absorption appears above the band gap energy ($E_g = 3.0$ eV[12]) and no absorption band is observed below E_g. The PC excitation spectrum also shows a rapid increase above E_g, because only above-band-gap excitation can generate photocarriers. The PC decreases above 3.1 eV, which is related to the dead layer near the surface. Anatase also shows an increase of PC above the band gap energy of 3.2 eV,[15] but the optical absorption has a long-tailed component below E_g, which may be attributed to shallow tail states below the band-gap energy. Both rutile and anatase show broad PL bands peaking at 2.9 and 2.5 eV, respectively. The broad PL spectrum shape and the large Stokes shift indicate that strongly localized states are involved in the PL processes in rutile and anatase. We have confirmed that the PL spectrum shapes in rutile and anatase are independent of the excitation light energy and intensity. It should be pointed out that the PL of rutile is only observed under strong pulse laser excitation, while anatase exhibits PL even under weak continuous-wave excitation, in spite of the indirect-gap band structure.

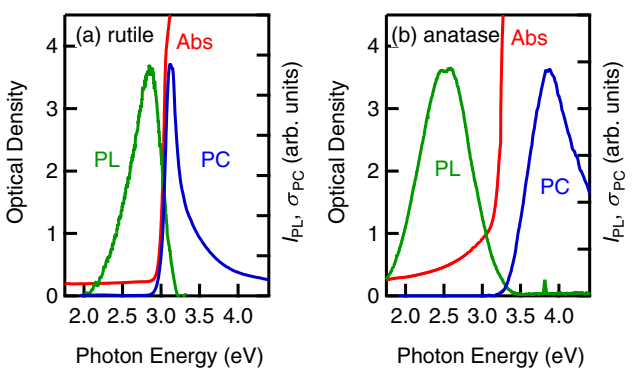

FIG. 1. Optical absorption (Abs), PL, and PC excitation spectra of (a) rutile and (b) anatase TiO_2 single crystals.

We begin with the discussion of photocarrier dynamics in rutile single crystals. Figure 2(a) shows the PL, TA, and PC intensities as a function of the excitation density I_{ex}. The PC and TA intensities linearly increase with excitation density, meaning that the photocarrier density is proportional to the excitation density and no nonlinear absorption occurs in these excitation densities. On the other hand, PL intensity shows a quadratic dependence on the excitation density in the range of 0.02–1.0 mJ/cm^2. This suggests that the broad blue PL intensity is determined by two-carrier recombination of photoexcited electrons and holes. Note that no exciton effects appear in the optical spectra of either rutile or anatase single crystals at room temperature. This is because of their high dielectric constants and small exciton binding energies,[14] and it indicates that band-to-band optical transitions dominate the optical processes in TiO_2 crystals.

Figure 2(b) shows the PL, PC, and TA decay profiles in rutile under an excitation of 50 μJ/cm^2. The PL decay curve shows a single exponential decay with a decay time of about 18 ns. The recombination processes of electrons and holes in semiconductors are usually expressed as a power series of the electron density n and hole density p.[21,22] Therefore, the rate equations for the photocarriers can be written simply as follows. The PL intensity at time t, $I_{PL}(t)$, of rutile is dominated by the following equations:

$$I_{PL}(t) \propto n(t)p(t), \tag{1a}$$

$$dn/dt = -n/\tau_n - Bnp - C_n n^2 p - C_p np^2, \tag{1b}$$

$$dp/dt = -p/\tau_p - Bnp - C_n n^2 p - C_p np^2, \tag{1c}$$

where $n(t)$ and $p(t)$ are the photoexcited electron and hole densities, respectively. τ_n and τ_p are the single-carrier nonradiative lifetimes for electrons and holes, respectively. B is the two-carrier radiative recombination coefficient. C_n and

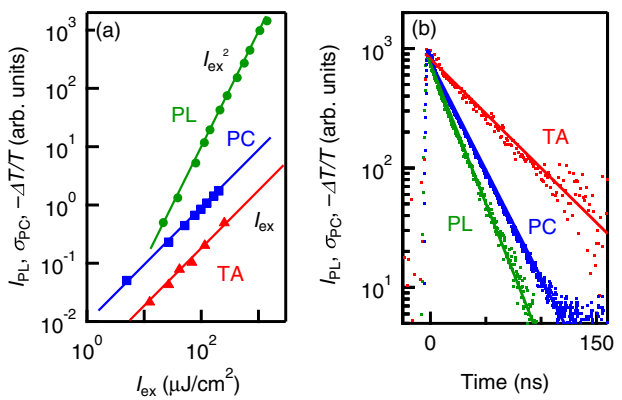

FIG. 2. (a) PL, PC, and TA signal intensities of rutile as a function of excitation density. (b) PL, PC, and TA decay profiles of rutile. Solid lines are curves fitted by a single exponential function. The lifetimes for PL, PC, and TA are 18, 24, and 48 ns, respectively.

C_p are the three-carrier Auger coefficients for electron–electron–hole and electron–hole–hole processes, respectively. Here, we can neglect the electron–hole radiative recombination term, Bnp, for our analyses, because the PL intensity is very weak and the radiative recombination rate is negligibly small in the forbidden-gap semiconductor rutile. In addition, Auger recombination usually causes the saturation of PL intensity under high excitation density, but no saturation behaviour is observed in Fig. 2(a). Therefore, we conclude that the Auger recombination is negligibly small under excitation below 1 mJ/cm^2. Note that the PL decay rate is the sum of the decay rates for electron and hole densities under low excitation density; according to Eqs. (1a)–(1c), we obtain

$$1/\tau_{PL} = 1/\tau_n + 1/\tau_p. \quad (2)$$

To determine the lifetimes for electrons and holes, we performed time-resolved PC and TA measurements. In Fig. 2(b), we plotted the PC decay dynamics of rutile. The PC decay curve shows a single exponential decay with a relaxation time of 24 ns. As shown in Fig. 2(a), the linear dependence of the photocurrent on the excitation density was confirmed in the range of excitation densities from 5 to 200 μJ/cm^2. The single exponential decay and linear power dependence indicate that multicarrier recombination processes, such as Auger recombination, and complicated transport processes are negligible at our experiential conditions. Because the mobility of electrons is much larger than that of holes in TiO_2, the PC of rutile and anatase TiO_2 is mainly contributed by electrons.[23] In addition, n-type photoconduction has been reported in rutile TiO_2.[24] Therefore, we conclude that the PC decay dynamics correspond to the decay dynamics for electron density, and we obtain $\tau_n \approx 24$ ns.

The TA decay curve also shows a single exponential decay with a decay time of 48 ns. The TA signal intensity linearly increases with increasing excitation density, as shown in Fig. 2(a). The intraband TA signal intensity is generally contributed by both photogenerated electrons and holes. The TA decay time is significantly different from the PC decay times, which correspond to the electron lifetime τ_n. Thus, we conclude that the TA signal in rutile is mainly contributed by the optical absorption from photoexcited holes. To check this conclusion, we calculated the PL lifetime according to Eq. (2) using electron and hole lifetimes derived from PC and TA dynamics, respectively. We obtained $\tau_{PL} \approx 16$ ns, which shows good agreement with the experimentally estimated time (18 ns). To summarize these results, we determined the electron and hole lifetimes in rutile consistently based on the combination of time-resolved PL, PC, and TA measurements.

Next, we discuss the photocarrier relaxation dynamics in anatase TiO_2 single crystals under the same experimental conditions. In Fig. 3(a), PL and TA decay curves of anatase in the nanosecond time region are plotted under an excitation density of 200 μJ/cm^2. PL and TA dynamics show complete agreement with each other. Considering that the TA signal corresponds to the hole density, this result indicates that both the PL and TA decay dynamics are determined by the hole lifetime: i.e., the hole lifetime is much shorter than the

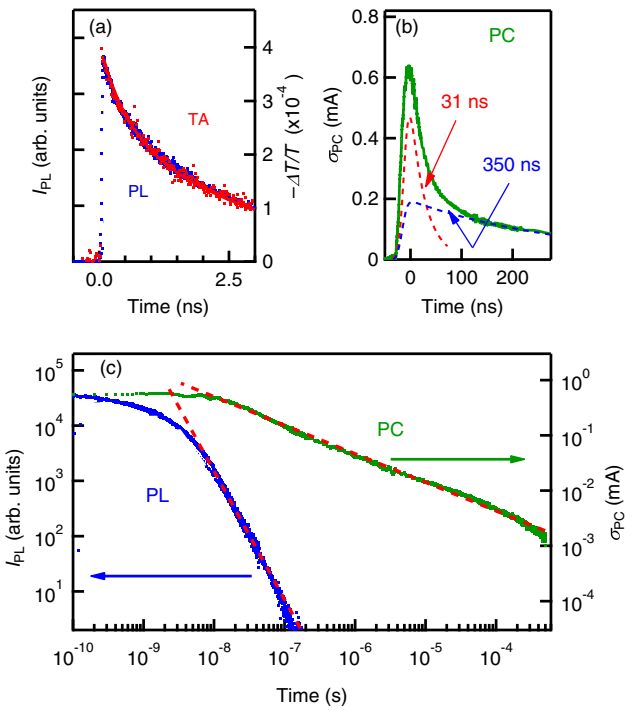

FIG. 3. (a) PL and TA decay dynamics of anatase in the nanosecond time window. (b) PC decay dynamics of anatase in the nanosecond time region. (c) PL and PC decay dynamics of anatase in a log–log plot.

electron lifetime. The decay curves show nonexponential profiles. We fitted the experimental curves in the range between 0 and 3.0 ns by a double exponential function, $I(t) = I_1\exp(-t/\tau_1) + I_2\exp(-t/\tau_2)$, and obtained the mean lifetime of holes, $\tau \approx 2.3$ ns, where τ is defined as $\tau = (I_1\tau_1 + I_2\tau_2)/(I_1 + I_2)$. Here, we checked that the PL and TA decay dynamics are insensitive to the excitation density at densities below 200 μJ/cm^2, meaning that the nonexponential decay profile is not due to two-carrier radiative recombination and three-carrier Auger recombination; rather, it is governed by single-carrier nonradiative decay processes [see Eqs. (1a)–(1c)]. These decay behaviors cannot be explained by the previous models based on two-carrier recombination.[25,26] Hereafter, we discuss the PL, PC, and TA decays in anatase under weak excitations below 200 μJ/cm^2.

Figure 3(b) shows the PC decay profile of anatase under an excitation of 40 μJ/cm^2 as a solid curve. The PC decays show nonexponential profiles. To estimate the PC lifetime, we fit the PC decay profiles by a Gaussian-convoluted double-exponential function in the range between −50 and 300 ns while taking the time resolution of the experimental setup (16 ns) into consideration. We obtained decay times of 31 ns and 350 ns, where the two exponential-decay components are plotted in the same figure as dotted curves. Apparently, the PC decay time is much longer than those of PL and TA. Because the PC dynamics correspond to the electron population dynamics, as mentioned above, these results suggest that the electron lifetime is much longer than the hole lifetime in anatase. This result is consistent with the previous report in powder samples.[23] Note that the long electron lifetime in anatase was also deduced from the PL and TA measurements. This indicates that the long electron lifetime is not dominated by the electron traps at the TiO_2/electrode interface.

Figure 3(c) shows the decay dynamics of PL and PC under the same excitation in a log–log plot. The PL dynamics obey a power-law scaling ($t^{-2.4}$) after 50 ns. The PC dynamics also show nonexponential decay, but PC shows a much longer lifetime ($\sim\mu$s) than PL dynamics. This means that the diffusion of long-lived electrons occurs in the microsecond time region, while the hole population rapidly decreases. These carrier decay dynamics in anatase are completely different from those in rutile. In anatase crystals, the interaction between electrons and holes is weak because of its indirect-gap band structure.

The power-law decay in the microsecond time region indicates the existence of multiple-trapping-dominated transport processes. It is known that the trapping of random-walking particles approximately obeys a power-law scaling, where the power index depends on the dimensionality and trapping process.[27–31] Thus, at present, we believe that multiple-trapping-dominated transport involving shallow tail states plays a role in the nonexponential decay of anatase. The dynamical properties are in good agreement with the larger luminescence Stokes shift and broader absorption tail of anatase shown in Fig. 1.

Finally, we consider the impact of carrier relaxation dynamics on photoactivity in rutile and anatase. Because of the long lifetime of electrons in anatase ($>1\ \mu$s), the electron diffusion reaches lengths of more than 10 μm, which is much longer than that of rutile ($\sim$100 nm), where we used the electron mobilities of 20 and 0.1 cm^2/Vs in rutile and anatase, respectively.[18] This will enhance the light–energy conversion efficiencies and photocatalytic reactivity in anatase, especially in bulk crystals and large volume samples. In the nanoparticles used in dye-sensitized solar cells and photocatalysts, the surface of the nanoparticles affects photocarrier dynamics because of the large surface-to-volume ratios in nanoparticles. The intrinsic bulk properties of the parent single crystals help to design the structures of nanocrystalline TiO_2-based optoelectronic devices.

In conclusion, we have studied the carrier recombination dynamics in rutile and anatase TiO_2 single crystals by combining PL, PC, and TA measurements. We revealed that the PC and TA dynamics correspond to the electron and hole decay dynamics, respectively. In rutile, the electrons and holes show exponential decays with lifetimes of 24 and 48 ns, respectively. On the other hand, anatase shows nonexponential decay profiles; electrons exist in the conduction band for more than a few microseconds, while holes rapidly decrease within a few nanoseconds. We discussed the carrier decay processes in rutile and anatase, and we pointed out that the long electron lifetime is related to the high photoactivity of anatase.

Part of this work was supported by KAKENHI (No. 20104006), The Sumitomo Electric Industries Group CSR Foundation, Kinki Invention Center, and JST-CREST.

[1]A. Fujishima and K. Honda, Nature **238**, 37 (1972).
[2]B. O'regan and M. Grätzel, Nature **353**, 737 (1991).
[3]R. Asahi, T. Morikawa, T. Ohwaki, K. Aoki, and Y. Taga, Science **293**, 269 (2001).
[4]S. In, A. Orlov, R. Berg, F. Garcia, S. Pedrosa-Jimenez, N. S. Tikhov, D. S. Wright, and R. M. Lambert, J. Am. Chem. Soc. **129**, 13790 (2007).
[5]G. Williams, B. Seger, and P. V. Kamat, ACS Nano **2**, 1487 (2008).
[6]J. R. Jennings, A. Ghicov, L. M. Peter, P. Schmuki, and A. B. Walker, J. Am. Chem. Soc. **130**, 13364 (2008).
[7]P. Roy, S. Berger, and P. Schmuki, Angew. Chem., Int. Ed. **50**, 2904 (2011).
[8]H. Tada, Q. Jin, H. Nishijima, H. Yamamoto, M. Fujishima, S. Okuoka, T. Hattori, Y. Sumida, and H. Kobayashi, Angew. Chem., Int. Ed. **50**, 3501 (2011).
[9]N.-G. Park, J. van de Lagemaat, and A. J. Frank, J. Phys. Chem. B **104**, 8989 (2000).
[10]S.-C. Li and D. Ulrike, J. Am. Chem. Soc. **132**, 64 (2010).
[11]J. Muscat, V. Swamy, and N. M. Harrison, Phys. Rev. B **65**, 224112 (2002).
[12]A. Sclafani and J. M. Herrmann, J. Phys. Chem. **100**, 13655 (1996).
[13]T. Hirakawa, K. Yawata, and Y. Nosaka, Appl. Catal., A **325**, 105 (2007).
[14]J. Pascual, J. Camassel, and H. Mathieu, Phys. Rev. B **18**, 5606 (1978).
[15]K. N. Glassford and J. R. Chelikowsky, Phys. Rev. B **46**, 1284 (1992).
[16]M. Emori, M. Sugita, K. Ozawa, and H. Sakama, Phys. Rev. B **85**, 035129 (2012).
[17]A. Atmout and R. Leonelli, Phys. Rev. B **51**, 6842 (1995).
[18]H. Tang, H. Prasad, R. Sanjinès, P. E. Schmid, and F. Lévy, J. Appl. Phys. **75**, 2042 (1994).
[19]C. Di Valentin and A. Selloni, J. Phys. Chem. Lett. **2**, 2223 (2011).
[20]N. Szydlo and R. Poirier, J. Appl. Phys. **51**, 3310 (1980).
[21]Y. Yamada and Y. Kanemitsu, Phys. Rev. B **82**, 113103 (2010).
[22]Y. Yamada, H. Yasuda, T. Tayagaki, and Y. Kanemitsu, Phys. Rev. Lett. **102**, 247401 (2009).
[23]K. M. Schnider and M. Kunst, J. Phys. Chem. **94**, 8222 (1990).
[24]N. Golego, S. A. Studenikin, and M. Cocivera, Phys. Rev. B **61**, 8262 (2000).
[25]R. Katoh, M. Murai, and A. Furube, Chem. Phys. Lett. **461**, 238 (2008).
[26]D. P. Colombo, Jr., K. A. Roussel, J. Saeh, D. E. Skinner, J. J. Cavaleri, and R. M. Bowman, Chem. Phys. Lett. **232**, 207 (1995).
[27]A. V. Barzykin and M. Tachiya, J. Phys. Chem. B **106**, 4356 (2002).
[28]J. Nelson, S. A. Haque, D. R. Klug, and J. R. Durrant, Phys. Rev. B **63**, 205321 (2001).
[29]J. Tang, J. R. Durrant, and D. R. Klug, J. Am. Chem. Soc. **130**, 13885 (2008).
[30]H. Scher and E. W. Montroll, Phys. Rev. B **12**, 2455 (1975).
[31]T. Tiedje and A. Rose, Solid State Commun. **37**, 49 (1981).